Tissue Thickness Effects on Radiometric Internal Body Temperature Measurements

Sofia Mvokany
Department of Electrical Engineering
University of Colorado Boulder
Boulder, CO, United States
Sofia.Mvokany@colorado.edu

Zoya Popović
Department of Electrical Engineering
University of Colorado Boulder
Boulder, CO, United States
zoya@colorado.edu

***Abstract*—This paper presents a study of the impact of tissue layer thicknesses on subcutaneous temperature measurements using microwave radiometry. A near-field antenna (NFA) is designed to receive black-body radiation from the brain when placed on top of six tissue layers of a human forehead. Each layer has a weighted contribution to the thermal noise power received by the NFA. In this paper, reciprocity is applied to computationally determine the weights of each layer which are needed to estimate the temperature. These weights depend on the tissue layer conductivities and thicknesses. The variation of tissue thicknesses between different body types result in different weights which affect the temperature measurement. It is found in simulations that for example maximizing skull thickness, results in an estimated temperature error of 0.82%.**

***Index Terms*—radiometry, core-body temperature, sensitivity analysis, bioelectromagnetics, weighting factors**

I. Introduction

Thermal regulation is a key physiological ability for human survival as a $\pm 3.5°$C deviation in internal temperature from the resting 37°C can lead to severe physiological impairments and even fatalities [1]. The ability to measure internal temperature is useful, e.g. during aortic repair surgery when the brain is in hypothermic hibernation at $15 - 20°$C for 30 minutes before it is gradually brought back to normal temperature [2], [3]. Throughout the procedure, the brain temperature is tracked through nasal catheters, however they lag compared to the true temperature. Other applications that benefit from the knowledge of internal temperature include hyperthermia treatment of cancers [4], diagnosis of sleep disorders, infections, etc. A variety of techniques have been used to monitor internal body temperature, such as thermometer pills [5], however, they are invasive and hard to track. Magnetic Resonance Imaging (MRI) [6] is expensive and non-wearable and heat-flux devices only measure about 1 cm of depth [7]. In this paper, microwave radiometry is used for internal body temperature measurements as it is a passive, compact and non-invasive measurement technique, illustrated in Fig. 1(a).

Microwave thermometry measures thermal black-body radiation emitted by any body above 0 K, to estimate temperature. It measures thermal noise power, emitted by the black body, across the electromagnetic spectrum. For humans, the spectral radiance peaks in the infrared range, however infrared frequencies penetrates only a few millimeters below the skin surface, limiting the sensing depth to the top skin layers only. In the microwave region of the spectrum, where penetration depth in tissues can be a few centimeters, the spectral power density of thermal radiation is directly proportional to temperature. For example, the penetration depth of a plane wave (classical skin depth) is 16.78 mm and 1.78 mm for skin conductivity at 1 and 10 GHz, respectively. For the case of fat and muscle, these values are (68.81,6.58) and (16.09,1.54), respectively.

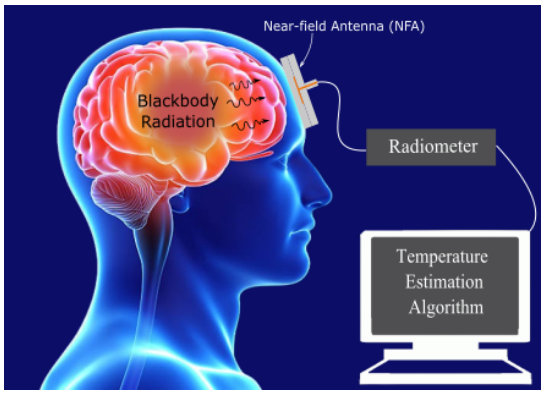

(a)

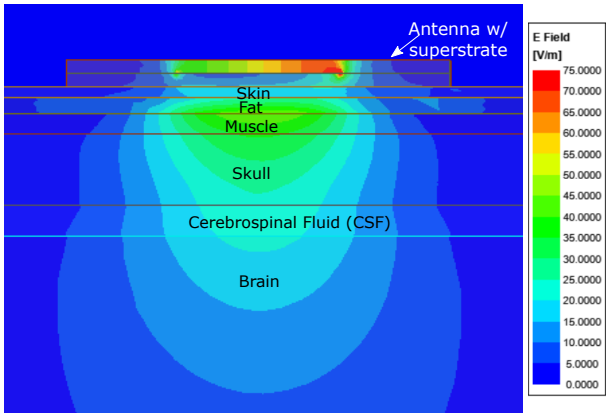

(b)

Fig. 1. (a) Microwave thermometry for measuring brain temperature with a near-field antenna (NFA) mounted on the skin on the forehead. (b) Example of a simulated electric field magnitude distribution within the tissue stack on the forehead.

In this work, we are using a radiometer, which is a sensitive receiver designed to have peaked responsitivity at 1.4 GHz to

measure thermal noise power emitted by sub-cutaneous tissue layers of a human forehead, illustrated in. Fig. 1(a), similar technique used in works such as [8], [9]. The temperature of the brain is then estimated from the total thermal power received by the near-field antenna (NFA) mounted on the skin. Fig. 1(b) shows the simulated E-field distribution at 1.4 GHz of the NFA within the six tissue layer stack of the forehead. A sensitivity analysis is carried out using Ansys HFSS to explore how the thicknesses of the tissues affect the estimated measured temperature of the brain. For a set of tissue thickness variations, the error in the temperature retrieval algorithm is computed for a healthy individual.

II. NFA Design and Weight Determination

From a radiometric measurement of the thermal noise power under the antenna in Fig. 1, the individual tissue layer temperatures can be found as a weighted sum from:

$$T_{tot} = \sum_{i=1}^{N} W_i(t_i, \sigma_i, \epsilon_r, f) \cdot T_i, \tag{1}$$

where T_i is the temperature of the i-th layer, and the weight W_i depends on the thickness t_i and electrical parameters of the layer. The thermal radiation can in principle be found using the fluctuation-dissipation theorem [10], but a more straightforward approach is to apply reciprocity and determine the absorption in each layer. The weights of the layers are defined as the percentage of volume Joule losses in a layer relative to losses in the entire tissue stack volume [8]:

$$W_i = \frac{P_i}{\sum_{i=1}^{N} P_i} \tag{2}$$

where P_i is the power dissipated in the i^{th} layer and the sum represents the total power dissipated in all the tissue layers in a finite volume under the NFA. The volume is truncated so that for 1 W of input power, only points where the power loss density values are larger than 10 W/m^3 are taken into account. Thus, the weights can be found numerically from full-wave simulations using Ansys HFSS, assuming the NFA is transmitting. It is also clear that the weights vary between different people, and this variation introduces errors in temperature estimation. To quantify the error, the antenna from Fig. 1 is modeled in the near field, placed on top of layered tissues tabulated in Table I, with thickness ranges encountered in male and female subjects found in the literature [11], [12], [13].

Fig.+- 2 shows the patch antenna topology and its measured and simulated reflection coefficient. The antenna is designed on Rogers 3010, chosen because of its high relative permittivity (10.2), allowing for reduced size. The patch is 16 mm by 29.43 mm on a 38 mm by 38 mm substrate. A superstrate helps match the NFA to the skin. The measured reflection coefficient agrees well with the simulated one for average tissue parameters of the forehead, and the measurement is repeatable. The measurement is done with a SOLT calibration to the reference plane of the SMA connector. Also shown in

TABLE I
Forehead Tissue Layers with Electrical Properties at 1.4 GHz and Thickness Range

Tissues	**(Relative permittivity ϵ_r, Conductivity σ(S/m))**	**Female Thickness Range (mm)**	**Male Thickness Range (mm)**
Skin	(39.7,1.04)	1.09-2.49	1.31-3.32
Fat	(5.4,0.06)	0.91-2.33	1.4-2.01
Muscle	(54.15,1.22)	0.5-3.45	0.71-2.93
Skull	(15.99,0.34)	5-11	5.5-9
CSF	(67.81,2.67)	1.73-2.6	1.73-2.6
Brain	(44.4,0.97)	90	90

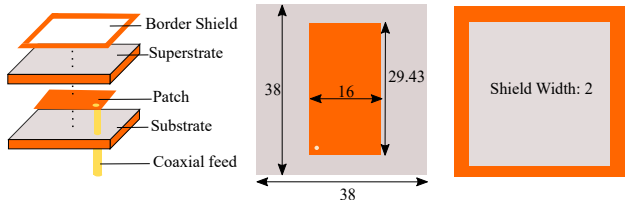

(a)

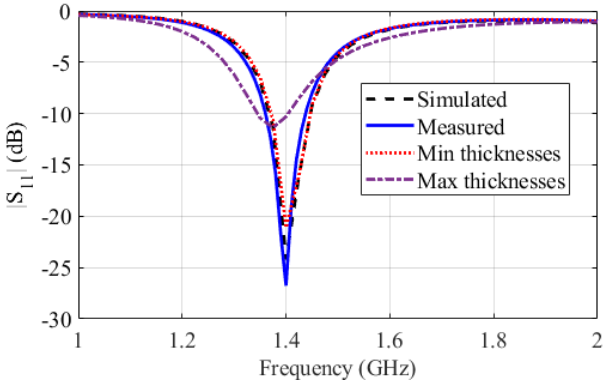

(b)

Fig. 2. (a) The near-field antenna is a metal patch on 38 mm×38 mm Rogers 3010 substrate and superstrate (ϵ_r =10.2, tanδ = 0.0022). All dimensions are given in mm. (b) Simulated and measured reflection coefficient of the NFA placed on the skin. The thicknesses of the tissues in the simulated case are 2, 1.7, 2, 7, 1.73 mm for skin, fat, muscle, skull and CSF respectively. The minimum and maximum thicknesses curves represent simulation data with general minimum (1.09, 0.91, 0.5, 5, 1.73 mm) and maximum t_i for each tissue layer (3.32, 2.33, 3.45, 11, 2.6 mm).

Fig. 2 is the simulated reflection coefficient for largest variation of tissue thicknesses among people. The goal of the NFA design is to maximize the weighting factor in the brain, as shown in Fig. 1(b), because this will result in the lowest error when estimating the brain temperature from the total noise power measurement.

Fig. 3 shows the volume Joule loss density for the 4 extremes cases of the thicknesses listed in Table I, illustrating how much the weights of the layers can vary depending on their thicknesses. It is also seen that the weights for

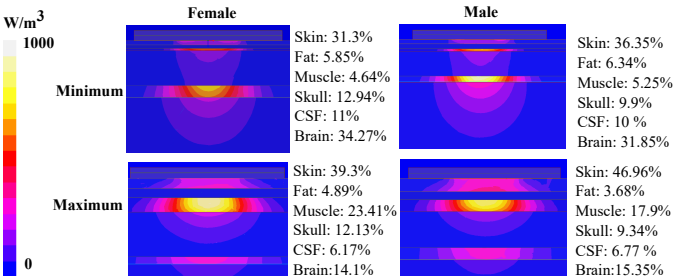

Fig. 3. Volume Joule loss density at within the tissue layers at 1.4 GHz, for minimum and maximum layer thicknesses in female and male subjects. Thicknesses from I. The weights for the individual tissues are also shown.

females and males vary significantly, e.g. at 1.4 GHz, the weight of the brain changes by 20.17% for females and 16.5% for males, between minimum and maximum thicknesses. To further quantify the effects of layer thicknesses on the weights, each layer thickness is varied, while the others are kept at commonly encountered values (2, 1.7, 2, 7, 1.7 mm for skin, fat muscle, skull and CSF respectively). This is repeated for each of the 5 layers above the brain. The weight of each layer is then computed with respect to each thickness sweep and the results for the female model are shown in Fig. 4.

Some conclusions can be drawn from Fig. 4. As mentioned previously, the weights depend on the electrical properties of the tissues, primarily their conductivity, as it governs the absorbed power in the medium. The higher the conductivity of the layer, the higher the absorption, leading to a larger weight value. This however is more relevant for layers that are closest to the surface, as opposed to buried layers. From 4, it is observed that the weight of the skin layer is consistently the highest as it is directly in contact with the NFA, and with σ and ϵ_r an order of magnitude higher than the fat layer directly below it. The fat layer weight stays below 8% for all combinations of tissue thicknesses considered here, maximized

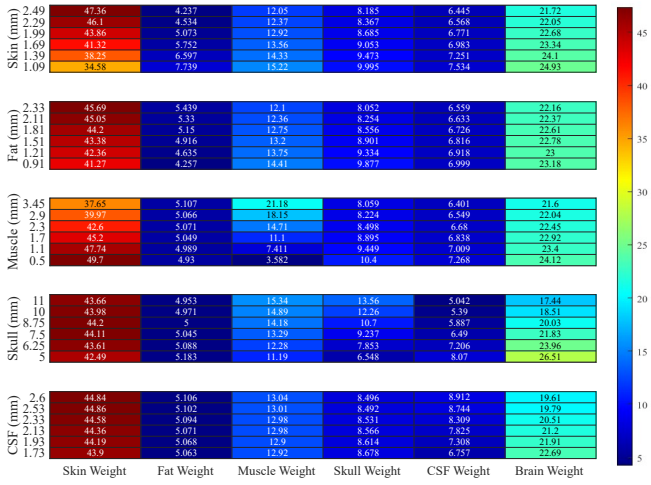

Fig. 4. 2-dimensional heat map generated using female subject thickness ranges, illustrating the effects of tissue thicknesses on the weights of the layers at 1.4 GHz.

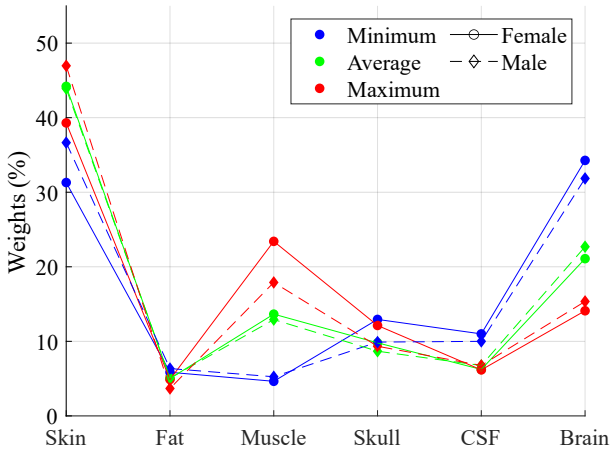

Fig. 5. Graphical representation of the weights of each tissue layer. Colors represent cases where the thicknesses are minimized (blue), averaged (green) and maximized (red). Line types correspond to females and males.

when the skin layer is the thinnest.

Interestingly, the muscle layer weight is the most impacted by its own thickness, as it is sandwiched between two layers with lower conductivity (fat and skull). The skull is the thickest layer of the stack, 10×thicker than the muscle layer when the tissue stack is minimized, and is observed to have the highest impact on the brain weight (17.44% for 11 mm thick to 26.51% for 5 mm thick when other layers are average). This is significant to highlight because studies have shown that, on average, females have frontal bones 1 mm thicker than males [14]. When the thickness of the skull is set to the average, the weight of the brain is computed to be around 20 to 25% across all sweeps, and the error in the temperature measurement will therefore be low.

Fig. 5 shows the difference in weights between the male and female models for three cases: (1) all layers of minimum thickness; (2) all layers of average; and (3) and all layers with maximum thickness. When observing the results for values in males, similarly to the female model, the weight of the brain is doubled when the stack thickness is minimized compared to the maximized case. In the thickest stack, 15.35% and 14.1% are obtained for weights of males and females, respectively, while weights of 31.85% and 34.27% are obtained for the thinnest stack.

III. Temperature Estimation and Error Percentage

Through a radiometric measurement, it is possible to retrieve the total thermal noise power T_{tot} emitted by a tissue stack, using (1), with W_i known from Fig. 4. This estimation was demonstrated in [8], [15] with an error as low as 0.25 K. This T_{tot} can be used to estimate the temperature of the brain T_{brain}, based on a few assumptions, such as the health conditions of the patient [16], no sudden temperature changes from one layer to another, whether thermal treatment (hypothermia or hyperthermia) is being applied on a specific layer at the

time of the measurement, etc. For the sake of this study, a healthy individual under no thermal treatment is assumed, with a "normal" temperature of the buried layers found in the literature [17] and the temperature of the superficial layers fitted assuming no sudden jump. The temperature of the layers from the skin to the brain are assumed to be between 36 and 39°C for the healthy individual.

Using weights plotted in Fig 5, the calculated T_{tot} for average tissue thicknesses is 37.06°C for a male, and 37.01°C for a female model. When the thicknesses are minimized, T_{tot} is 37.3°C for the male and 37.4°C for the female model. When they are maximized, T_{tot} is 36.88°C in males and 36.90°C in females.

To quantify the error in computing T_{brain} using the simulated weights, we assume $T_{tot} = 37$°C, shown in Table II. For a healthy individual, T_{brain} for an average female tissue stack is estimated to be 38.9°C, a 0.1 °C (0.25%) difference from the actual brain temperature of 39°C. Assuming a minimized stack for a total temperature of $T_{tot} = 37$°C, the error is higher, 0.4 °C (about 3%), because the actual $T_{tot} = 37.4$°C in this case.

TABLE II
ERROR PERCENTAGE FOR NORMAL BRAIN TEMPERATURE (39°C) IF T_{tot}=37°C

Tissue Stack	**Computed T_{brain}(°C)**	**Estimation Error(%)**
Average female	38.9	0.25
Average male	38.75	0.64
11 mm skull	39.32	0.82
3.32 mm muscle	39.21	0.54
Minimized female stack	37.82	3.02
Maximized male stack	39.78	2

IV. CONCLUSIONS

In conclusion, this paper studies the effects of tissue thicknesses on internal temperature measurements using microwave thermometry. A near field antenna (NFA) is designed to receive thermal noise power from a six-layer tissue stack representing a human forehead. The weighted thermal contribution of each of the layers present in the stack is computed using electromagnetic reciprocity. The weights depend on the electrical properties of the tissues and their thicknesses. To retrieve the temperature of the brain, the NFA is designed to maximize its weight in the brain tissue. Using Ansys HFSS, the weights of each layer are computed using a realistic thickness range in a female and male model. The skull thickness is found to have the most impact on the weight of the brain. The final conclusion from the simulations is that, assuming a calibrated radiometer, the error in brain temperature estimation is small (less than a percent) when the thicknesses of the skin, fat, muscle, skull and CSF vary within statistical measured values.

ACKNOWLEDGMENT

This work was supported by NSF grants IIP2044668 (PFI-TT) and ECCS202652.

REFERENCES

[1] C. L. Lim, C. Byrne, and J. K. Lee, "Human thermoregulation and measurement of body temperature in exercise and clinical settings," *Annals Academy of Medicine Singapore*, vol. 37, no. 4, p. 347, 2008.

[2] E. Dumont, M. Carrier, R. Cartier, M. Pellerin, N. Poirier, D. Bouchard, and L. P. Perrault, "Repair of aortic false aneurysm using deep hypothermia and circulatory arrest," *The Annals of thoracic surgery*, vol. 78, no. 1, pp. 117–120, 2004.

[3] R. B. Griepp and G. Di Luozzo, "Hypothermia for aortic surgery," *The Journal of Thoracic and Cardiovascular Surgery*, vol. 145, no. 3, pp. S56–S58, 2013.

[4] P. K. Sneed, P. R. Stauffer, M. W. McDermott, C. J. Diederich, K. R. Lamborn, M. D. Prados, S. Chang, K. A. Weaver, L. Spry, M. K. Malec *et al.*, "Survival benefit of hyperthermia in a prospective randomized trial of brachytherapy boost±hyperthermia for glioblastoma multiforme," *International Journal of Radiation Oncology* Biology* Physics*, vol. 40, no. 2, pp. 287–295, 1998.

[5] C. C. Bongers, M. T. Hopman, and T. M. Eijsvogels, "Using an ingestible telemetric temperature pill to assess gastrointestinal temperature during exercise," *JoVE (Journal of Visualized Experiments)*, no. 104, p. e53258, 2015.

[6] G. Galiana, R. T. Branca, E. R. Jenista, and W. S. Warren, "Accurate temperature imaging based on intermolecular coherences in magnetic resonance," *Science*, vol. 322, no. 5900, pp. 421–424, 2008.

[7] Y. Eshraghi, V. Nasr, I. Parra-Sanchez, A. Van Duren, M. Botham, T. Santoscoy, and D. I. Sessler, "An evaluation of a zero-heat-flux cutaneous thermometer in cardiac surgical patients," *Anesthesia & Analgesia*, vol. 119, no. 3, pp. 543–549, 2014.

[8] P. Momenroodaki, W. Haines, M. Fromandi, and Z. Popovic, "Noninvasive internal body temperature tracking with near-field microwave radiometry," *IEEE Transactions on Microwave Theory and Techniques*, vol. 66, no. 5, pp. 2535–2545, 2017.

[9] S. G.Vesnin et al., "Portable microwave radiometer for wearable devices," *Sensors and Actuators A: Physical*, vol. 318, p. 112506, 2021.

[10] I. Karanasiou, N. Uzunoglu, and C. Papageorgiou, "Towards functional noninvasive imaging of excitable tissues inside the human body using focused microwave radiometry," *IEEE Transactions on Microwave Theory and Techniques*, vol. 52, no. 8, pp. 1898–1908, 2004.

[11] B. S. F. Bravo, R. de Melo Carvalho, L. Penedo, J. T. de Bastos, M. Calomeni Elias, S. Cotofana, K. Frank, N. Moellhoff, L. Freitag, and M. Alfertshofer, "Applied anatomy of the layers and soft tissues of the forehead during minimally-invasive aesthetic procedures," *Journal of Cosmetic Dermatology*, vol. 21, no. 11, pp. 5864–5871, 2022.

[12] N. Kulathunga, A. Vadysinghe, M. Sivasubramanium, K. Ekanayake, and Y. Wijesiriwardena, "Variation of the human skull bone thickness with the age, gender, and body stature: an autopsy study of the Sri Lankan population," *Medico-Legal Journal of Sri Lanka*, vol. 10, no. 1, 2022.

[13] W. Snyder, M. Cook, E. Nasset, L. Karhausen, and I. Tipton, "Report of the task group on reference man," *Report Prepared for International Commission on Radiological Protection*, no. 23, pp. 46–57.

[14] M. S. Eksi, M. Güdük, and M. I. Usseli, "Frontal bone is thicker in women and frontal sinus is larger in men: A morphometric analysis," *Journal of Craniofacial Surgery*, vol. 32, no. 5, pp. 1683–1684, 2021.

[15] J. Lee, G. S. Botello, R. Streeter, and Z. Popović, "A 1.4-GHz GaAs MMIC radiometer for noninvasive internal body thermometry," *IEEE Transactions on Microwave Theory and Techniques*, 2023.

[16] B. Yulug, H. A. Velioglu, D. Sayman, S. Cankaya, and L. Hanoglu, "Brain temperature in healthy and diseased conditions: A review on the special implications of mrs for monitoring brain temperature," *Biomedicine Pharmacotherapy*, vol. 160, p. 114287, 2023. [Online]. Available: https://www.sciencedirect.com/science/article/pii/S0753332223000756

[17] N. M. Rzechorzek, M. J. Thrippleton, F. M. Chappell, G. Mair, A. Ercole, M. Cabeleira, C.-T. H. R. I. H. I. S.-S. Participants, Investigators, J. Rhodes, I. Marshall, and J. S. O'Neill, "A daily temperature rhythm in the human brain predicts survival after brain injury," *Brain*, vol. 145, no. 6, pp. 2031–2048, 2022.